

SEL: A Fully-Implicit, Parallel Spectral Element Fluid Simulation Code

Alan H. Glasser



Collaborators:

V. S. Lukin, V. D. Liseikin

Presented at
Future Directions for M3D, PPPL
Princeton, NJ, March 20, 2007

SEL Code Features

- Advanced Fortran 95.
- Flux-source form: simple, general problem setup.
- Spatial discretization:
 - High-order C^0 spectral elements, modal basis
 - Harmonic grid generation, adaptation, alignment
- Time step: fully implicit, 2nd-order accurate,
 - θ -scheme
 - BDF2
- Static condensation, Schur complement.
 - Small local direct solves for grid cell interiors.
 - Preconditioned GMRES for Schur complement.
- Distributed parallel operation with MPI and PETSc.

Spatial Discretization

Flux-Source Form of Equations

$$\frac{\partial u^i}{\partial t} + \nabla \cdot \mathbf{F}^i = S^i$$

$$\mathbf{F}^i = \mathbf{F}^i(t, \mathbf{x}, u^j, \nabla u^j)$$

$$S^i = S^i(t, \mathbf{x}, u^j, \nabla u^j)$$

Galerkin Expansion

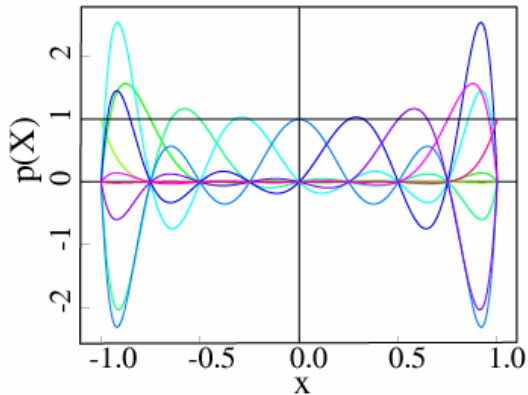
$$u^i(t, \mathbf{x}) \approx \sum_{j=0}^n u_j^i(t) \alpha_j(\mathbf{x})$$

Weak Form of Equations

$$(\alpha_i, \alpha_j) \dot{u}_j^k = \int_{\Omega} d\mathbf{x} \left(S^k \alpha_i + \mathbf{F}^k \cdot \nabla \alpha_i \right) - \int_{\partial\Omega} d\mathbf{x} \alpha_i \mathbf{F}^k \cdot \hat{\mathbf{n}}$$

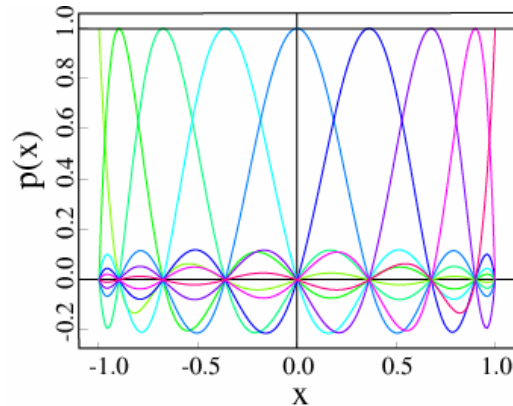
Alternative Polynomial Bases

Uniform Nodal Basis



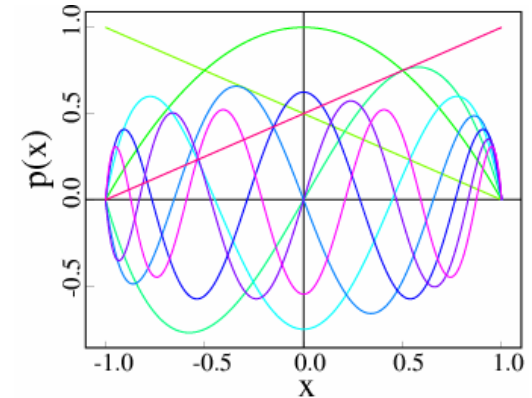
- Lagrange interpolatory polynomials
- Uniformly-spaced nodes
- Diagonally subdominant

Jacobi Nodal Basis



- Lagrange interpolatory polynomials
- Nodes at roots of $(1-x^2) P_n^{(0,0)}(x)$
- Diagonally dominant

Spectral (Modal) Basis



- Jacobi polynomials $(1+x)/2$, $(1-x)/2$, $(1-x^2) P_n^{(1,1)}(x)$
- Nearly orthogonal
- Manifest exponential convergence

Implicit Time Discretization: θ -Scheme

$$\mathbf{M}\dot{\mathbf{u}} = \mathbf{r}$$

$$\mathbf{M} \left(\frac{\mathbf{u}^+ - \mathbf{u}^-}{h} \right) = \theta \mathbf{r}^+ + (1 - \theta) \mathbf{r}^-$$

$$\mathbf{R}(\mathbf{u}^+) \equiv \mathbf{M}(\mathbf{u}^+ - \mathbf{u}^-) - h[\theta \mathbf{r}^+ + (1 - \theta) \mathbf{r}^-] \rightarrow 0$$

$$\mathbf{J} \equiv \mathbf{M} - h\theta \left\{ \begin{array}{c} \frac{\partial r_i^+}{\partial u_j^+} \end{array} \right\}$$

$$\mathbf{R}(\mathbf{u}^+) + \mathbf{J}\delta\mathbf{u}^+ = \mathbf{0}, \quad \delta\mathbf{u}^+ = -\mathbf{J}^{-1}\mathbf{R}(\mathbf{u}^+), \quad \mathbf{u}^+ \rightarrow \mathbf{u}^+ + \delta\mathbf{u}^+$$

- Nonlinear Newton-Krylov iteration.
- Elliptic equations: $\mathbf{M} = 0$.
- Static condensation
- PETSc: GMRES with Schwarz ILU, overlap of 3, fill-in of 5.

Static Condensation

Partition into Subdomains (Grid Cells) Ω_i

I : Interiors

Γ : Interface: (faces) + edges + vertices.

Block Matrix Form

$$\mathbf{L}\mathbf{u} = \mathbf{r}, \quad \mathbf{L} = \begin{pmatrix} \mathbf{L}_{II} & \mathbf{L}_{I\Gamma} \\ \mathbf{L}_{\Gamma I} & \mathbf{L}_{\Gamma\Gamma} \end{pmatrix}, \quad \mathbf{u} = \begin{pmatrix} \mathbf{u}_I \\ \mathbf{u}_\Gamma \end{pmatrix}, \quad \mathbf{r} = \begin{pmatrix} \mathbf{r}_I \\ \mathbf{r}_\Gamma \end{pmatrix}$$

Solution for \mathbf{u}_I

$$\mathbf{u}_I = \mathbf{L}_{II}^{-1} (\mathbf{r}_I - \mathbf{L}_{I\Gamma} \mathbf{u}_\Gamma)$$

Schur Complement

$$\mathbf{S} \equiv \mathbf{L}_{\Gamma\Gamma} - \mathbf{L}_{\Gamma I} \mathbf{L}_{II}^{-1} \mathbf{L}_{I\Gamma}, \quad \mathbf{S} \mathbf{u}_\Gamma = \mathbf{r}_\Gamma - \mathbf{L}_{\Gamma I} \mathbf{L}_{II}^{-1} \mathbf{r}_I$$

- \mathbf{L}_{II}^{-1} : small local direct solves, LU factorization and back substitution.
- \mathbf{S}^{-1} : global solve, preconditioned GMRES.

The Benefits of Static Condensation

nx = number of grid cells in x direction

ny = number of grid cells in y direction

np = degree of polynomials in x and y

$nqty$ = number of physical quantities

N = order of global matrix to be solved

Without static condensation: $N = nx ny nqty np^2$

With static condensation: $N = nx ny nqty (2 np - 1)$

Surface to volume ratio.

Substantial reduction of condition number.

The Need for a 3D Adaptive Field-Aligned Grid

- An essential feature of magnetic confinement is very strong anisotropy, $\chi_{||} \gg \chi_{\perp}$.
- The most unstable modes are those with $k_{||} \approx 1/R < 1/a \approx k_{\perp}$.
- The most effective numerical approach to these problems is a field-aligned grid packed in the neighborhood of singular surfaces and magnetic islands. NIMROD.
- Long-time evolution of helical instabilities requires that the packed grid follow the moving perturbations into 3D.
- Multidimensional oblique rectangular AMR grid is larger than necessary and does not resolve anisotropy.
- Novel algorithms must be developed to allow alignment of the grid with the dominant magnetic field and automatic grid packing normal to this field.
- Such methods must allow for regions of magnetic islands and stochasticity.

Methods of Adaptive Gridding

Adaptive Mesh Refinement

1. Coarse and fine patches of rectangular grid.
2. Complex data structures.
3. Oblique to magnetic field.
4. Static regrid.
5. Explicit time step; implicit a research problem.
6. Berger, Gombosi, Colella, Samtaney, Jardin

Harmonic Grid Generation

1. Harmonic mapping of rectangular grid onto curvilinear grid.
2. Logically rectangular
3. Aligned with magnetic field.
4. Static or dynamic regrid.
5. Explicit or implicit time step.
6. Liseikin, Winslow, Dvinsky, Brackbill, Knupp

Adaptive Grid Kinematics: How to Use Logical Coordinates.

$$x^j(\xi^k) = \sum_i x_i^j \alpha_i(\xi^k), \quad j, k = 1, 2$$

$$\mathcal{J} \equiv (\hat{\mathbf{z}} \cdot \nabla \xi^1 \times \nabla \xi^2)^{-1} = \frac{\partial x^1}{\partial \xi^1} \frac{\partial x^2}{\partial \xi^2} - \frac{\partial x^1}{\partial \xi^2} \frac{\partial x^2}{\partial \xi^1}$$

$$\frac{\partial u^k}{\partial t} + \nabla \cdot \mathbf{F}^k = S^k, \quad \frac{\partial u^k}{\partial t} + \frac{1}{\mathcal{J}} \frac{\partial}{\partial \xi^j} (\mathcal{J} \mathbf{F}^k \cdot \nabla \xi^j) = S^k$$

$$u^k(t, \mathbf{x}) \approx \sum_{j=0}^n u_j^k(t) \alpha_j(\xi), \quad (u, v) \equiv \int_{\Omega} u v d\mathbf{x} = \int_{\Omega} u v \mathcal{J} d\xi$$

$$(\alpha_i, \alpha_j) \dot{u}_j^k = \int_{\Omega} \left(S^k \alpha_i + \mathbf{F}^k \cdot \nabla \xi^j \frac{\partial \alpha_i}{\partial \xi^j} \right) \mathcal{J} d\xi - \int_{\partial \Omega} \alpha_i \mathbf{F}^k \cdot \hat{\mathbf{n}} \mathcal{J} d\xi$$

Adaptive Grid Dynamics: How to Choose Logical coordinates.

$$\mathcal{L} \equiv \frac{1}{2} \int \left[(\mathbf{B} \cdot \nabla \xi^j)^2 + \epsilon |\nabla \xi^j|^2 \right] d\mathbf{x}$$

$$\frac{\delta \mathcal{L}}{\delta \xi^j} = 0 \Rightarrow \nabla \cdot (\mathbf{g} \cdot \nabla \xi^j) = 0, \quad \mathbf{g} \equiv \mathbf{B}\mathbf{B} + \epsilon \mathbf{I}$$

Beltrami equation + boundary conditions \Rightarrow logical coordinates.
 Alignment with magnetic field except where $\mathbf{B} \rightarrow 0$, isotropic term dominates.

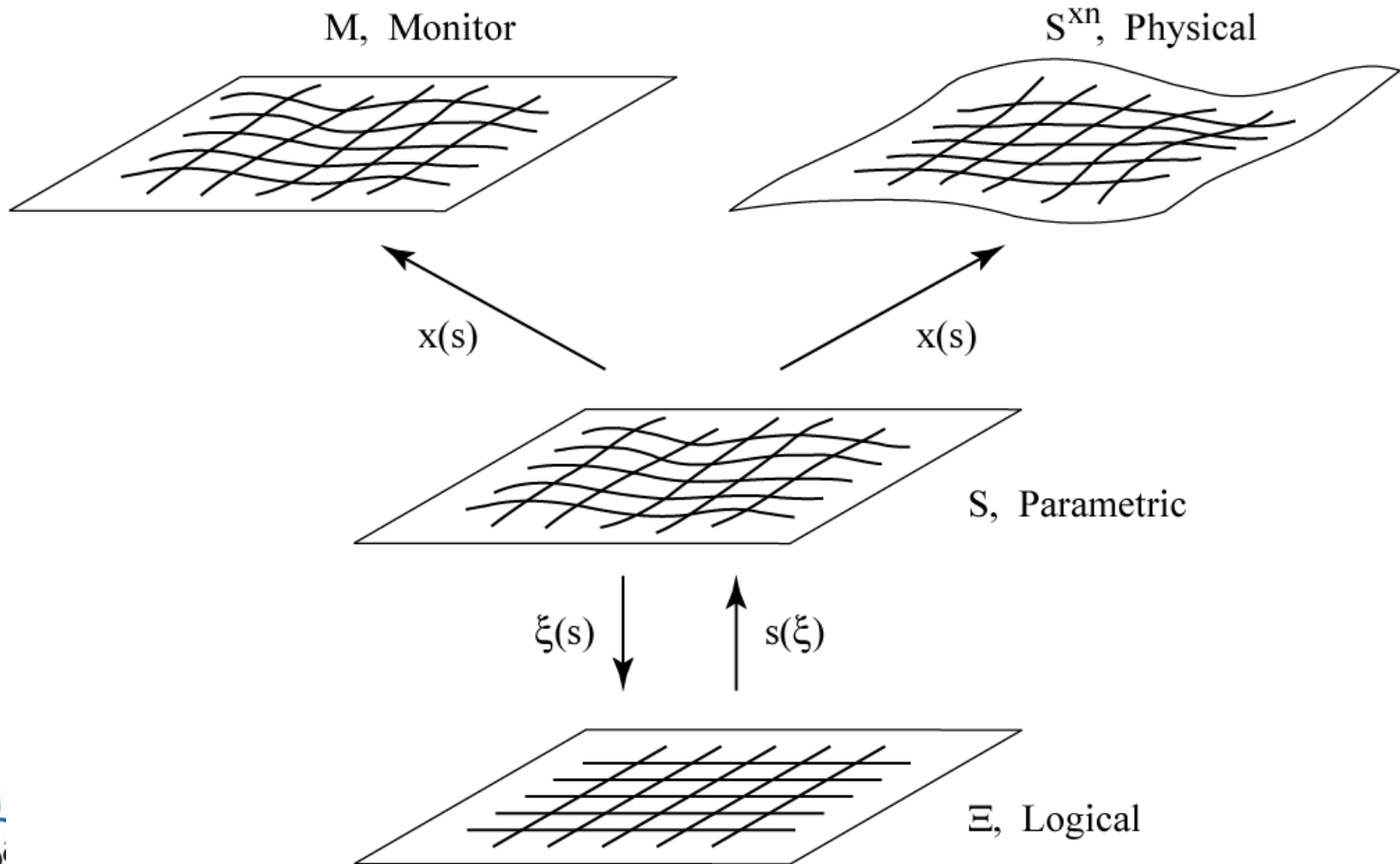
Vladimir D. Liseikin

A Computational Differential Geometry Approach to Grid Generation

Springer Series in Synergetics, 2003

Domains and Transformations

Used in Harmonic Grid Generation



UNCLASSIFIED

Slide 11

Modified Beltrami Equation

Variational Principle

$$\mathcal{L} = \frac{1}{2} \int_{\Omega} \frac{1}{w\sqrt{g}} \mathbf{g} : \nabla \xi^i \nabla \xi^i dx$$

Euler-Lagrange Equation

$$\nabla \cdot \left(\frac{1}{w\sqrt{g}} \mathbf{g} \cdot \nabla \xi^i \right) = 0$$

Expressed in Logical Coordinates

$$\frac{1}{\mathcal{J}} \frac{\partial}{\partial \xi^j} \left(\frac{\mathcal{J}}{w\sqrt{g}} g^{kl} \frac{\partial \xi^i}{\partial x^k} \frac{\partial \xi^j}{\partial x^l} \right) = 0, \quad \frac{\partial \xi^i}{\partial x^j} \rightarrow \frac{\partial x^i}{\partial \xi^j}$$

Two-Fluid Extended MHD Equations

$$\frac{\partial \rho}{\partial t} + \nabla \cdot (\rho \mathbf{v}_i) = 0$$

$$\frac{\partial(\rho \mathbf{v}_i)}{\partial t} + \nabla \cdot \mathbf{T}_i = 0$$

$$\mathbf{T}_i \equiv \rho \mathbf{v}_i \mathbf{v}_i + p \mathbf{I} + (B^2/2) \mathbf{I} - \mathbf{B} \mathbf{B} - \bar{\mu} (\nabla \mathbf{v}_i + \nabla \mathbf{v}_i^T) - \bar{\nu} \nabla (v_{ez} \hat{z})$$

$$\mathbf{E} = -\mathbf{v}_e \times \mathbf{B} - \frac{d_i}{\rho} \nabla p_e + \bar{\eta} \mathbf{J} + \frac{d_i}{\rho} \bar{\nu} \nabla^2 (v_{ez} \hat{z})$$

$$\begin{aligned} \frac{1}{\gamma - 1} \frac{\partial p}{\partial t} + \nabla \cdot \left(\frac{\gamma}{\gamma - 1} p \mathbf{v}_i - \bar{\kappa}_\perp \nabla_\perp T - \bar{\kappa}_\parallel \nabla_\parallel T \right) \\ = \mathbf{v}_i \cdot \nabla p + \bar{\eta} |\mathbf{J}|^2 + \bar{\mu} (\nabla \mathbf{v}_i + \nabla \mathbf{v}_i^T) : \nabla \mathbf{v}_i + \bar{\nu} |\nabla v_{ez}|^2 \end{aligned}$$

$$d_i \nabla \times \mathbf{B} = d_i \mathbf{J} = \rho \mathbf{v}_i - \rho \mathbf{v}_e, \quad \frac{\partial \mathbf{B}}{\partial t} = -\nabla \times \mathbf{E}$$

$$p = p_i + p_e = \rho T = \rho (T_i + T_e), \quad \frac{T_e}{T_i} = \alpha$$

GEM Challenge Problem

Dimensionless Parameter Definitions and Values

$$d_i \equiv \frac{c/\omega_{pi}}{L_0} = 1, \quad \alpha = 0.2$$

$$\bar{\eta} \equiv \frac{\eta c^2}{L_0 B_0} \left(\frac{n_0 m_i}{4\pi} \right)^{1/2} = 5 \times 10^{-3}$$

$$\bar{\mu} \equiv \frac{\mu_i}{L_0 B_0} \left(\frac{4\pi m_i}{n_0} \right)^{1/2} = 5 \times 10^{-2}$$

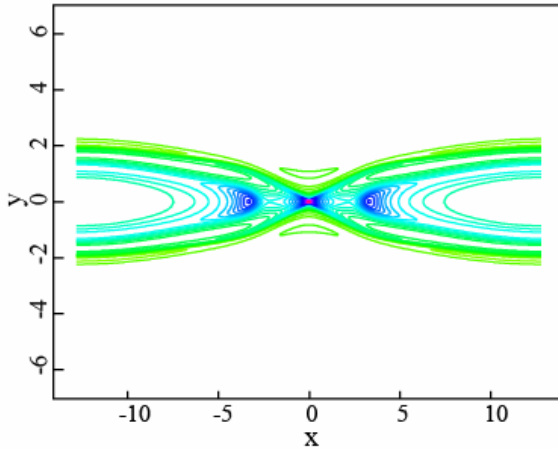
$$\bar{\nu} \equiv \frac{\mu_e}{L_0 B_0} \left(\frac{4\pi}{n_0 m_i} \right)^{1/2} = 5 \times 10^{-6}$$

$$\bar{\kappa}_{\parallel} \equiv \frac{\kappa_{\parallel}}{L_0 B_0} \left(\frac{4\pi m_i}{n_0} \right)^{1/2} = 2 \times 10^{-2}$$

$$\bar{\kappa}_{\perp} \equiv \frac{\kappa_{\perp}}{L_0 B_0} \left(\frac{4\pi m_i}{n_0} \right)^{1/2} = 2 \times 10^{-2}$$

Contour Plots

Electron z-momentum at $t = 20.0625$



$$\nu = 1 * 10^{-5}$$

Logical grid:

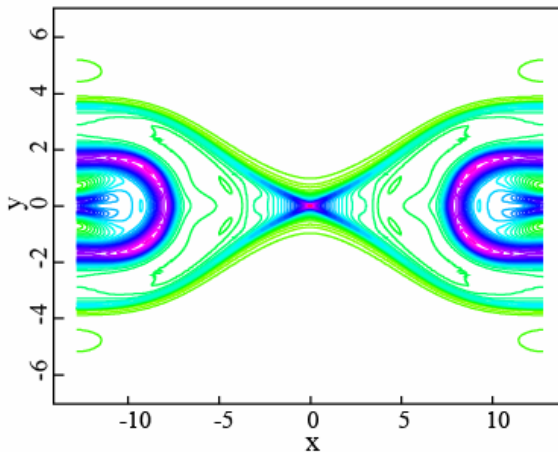
$$[n_x, n_y, n_p] = [40, 40, 8]$$

of time-steps = 419

$$dt = .0625 \rightarrow .25$$

of grid remappings = 18

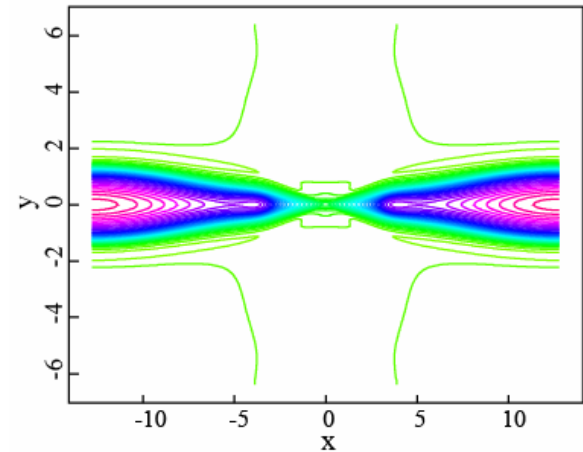
Electron z-momentum at $t = 29.125$



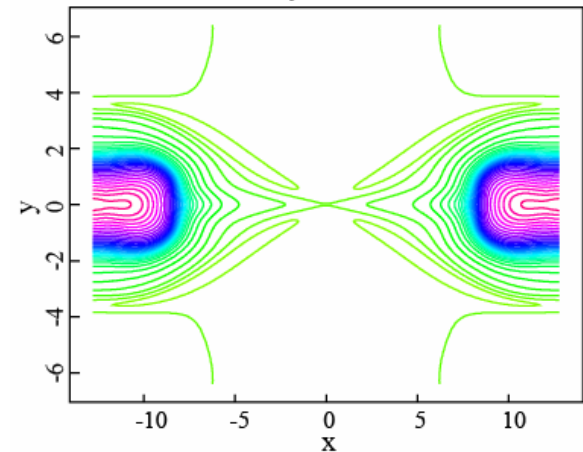
Computed on Bassi
4 nodes x 8 processors

Wallclock time = 9 hours
 \Rightarrow cpu time = 288 hours

Density at $t = 20.0625$

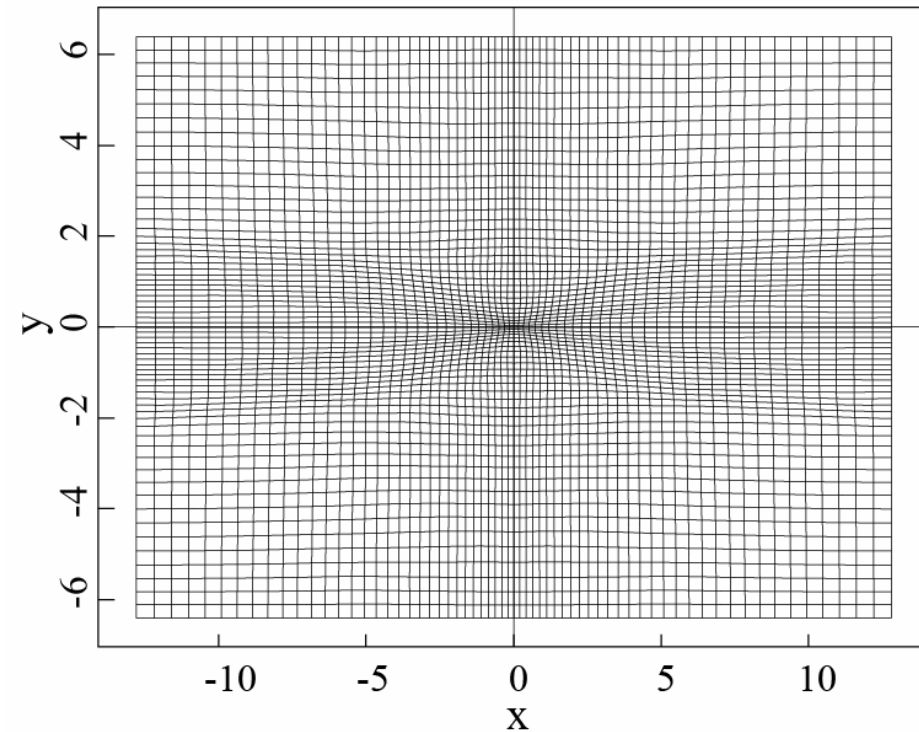


Density at $t = 29.125$

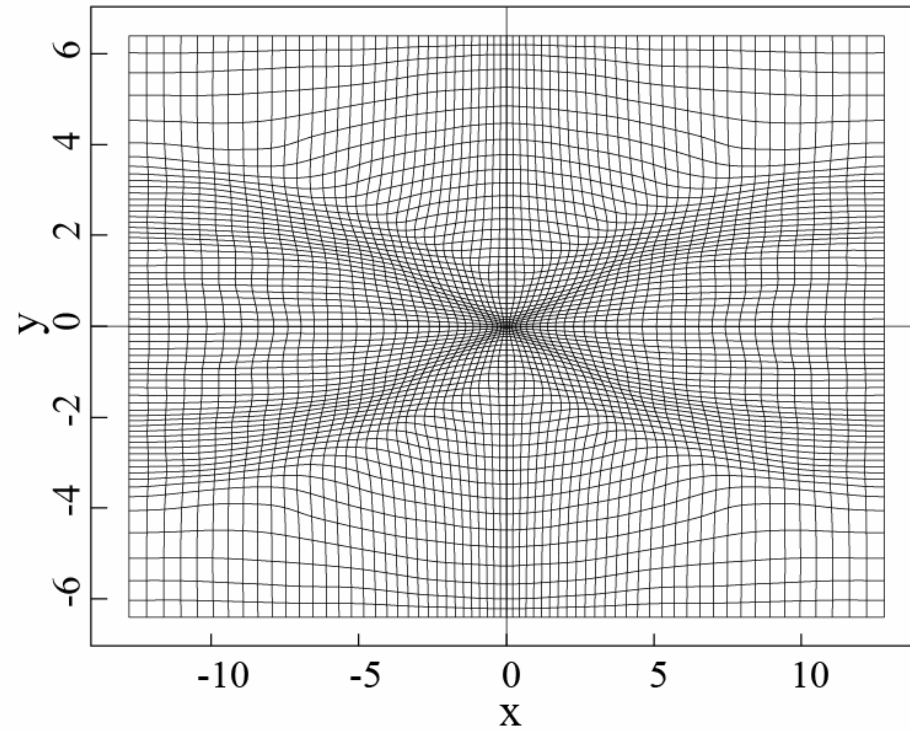


Computational Grids

Peak of Reconnection Rate, $t = 20.0625$



Peak of Kinetic Energy, $t = 20.0625$

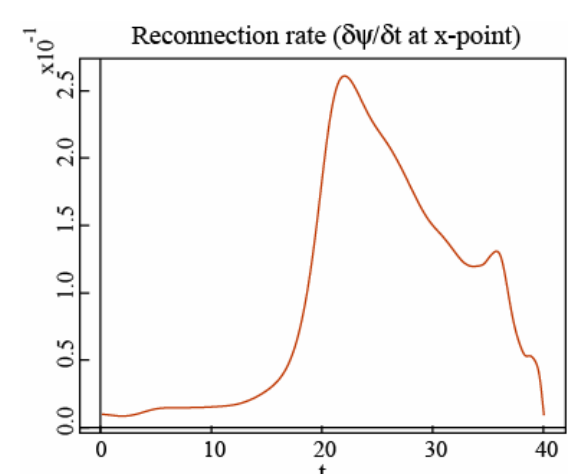
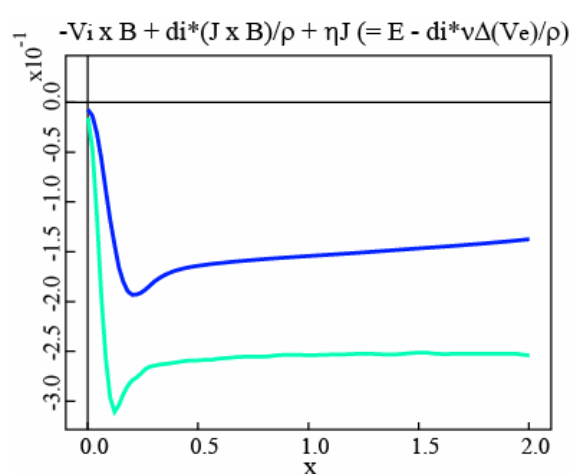
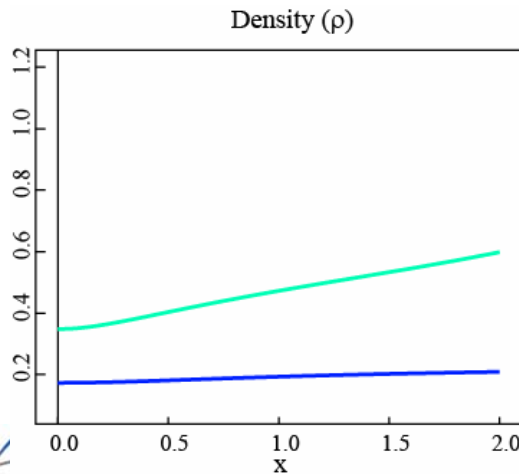
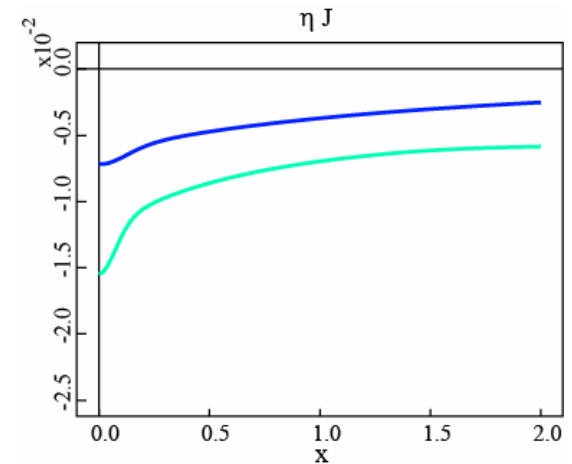
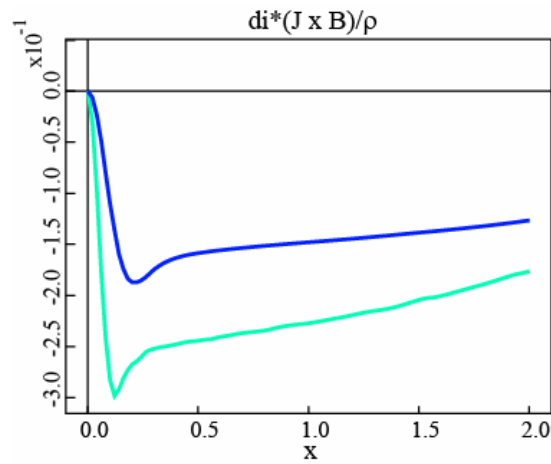
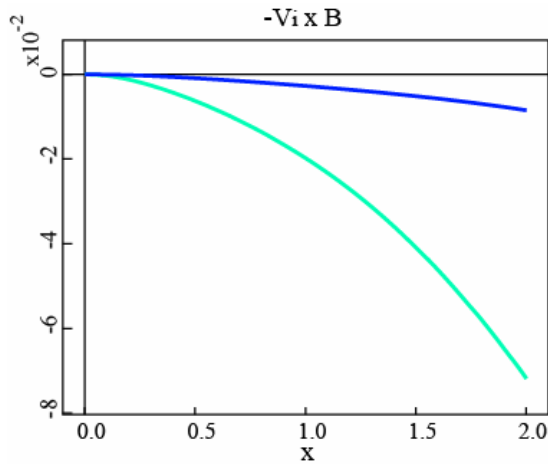


Cut at mid-plane
(x-axis in units of d_j)

Slice Plots

— $t = 20.0625$
(peak of reconnection rate)

— $t = 29.125$
(peak of kinetic energy)

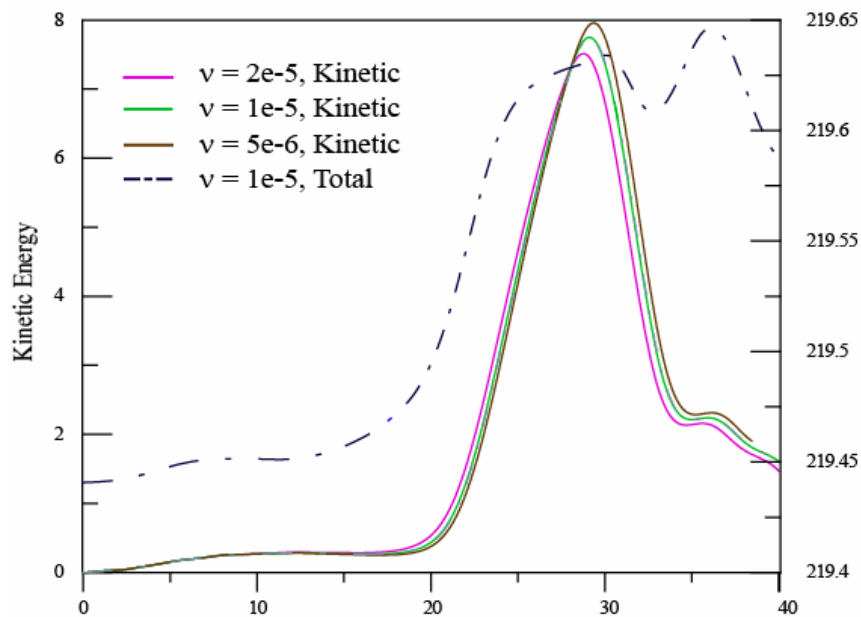


Time-Dependent Diagnostics

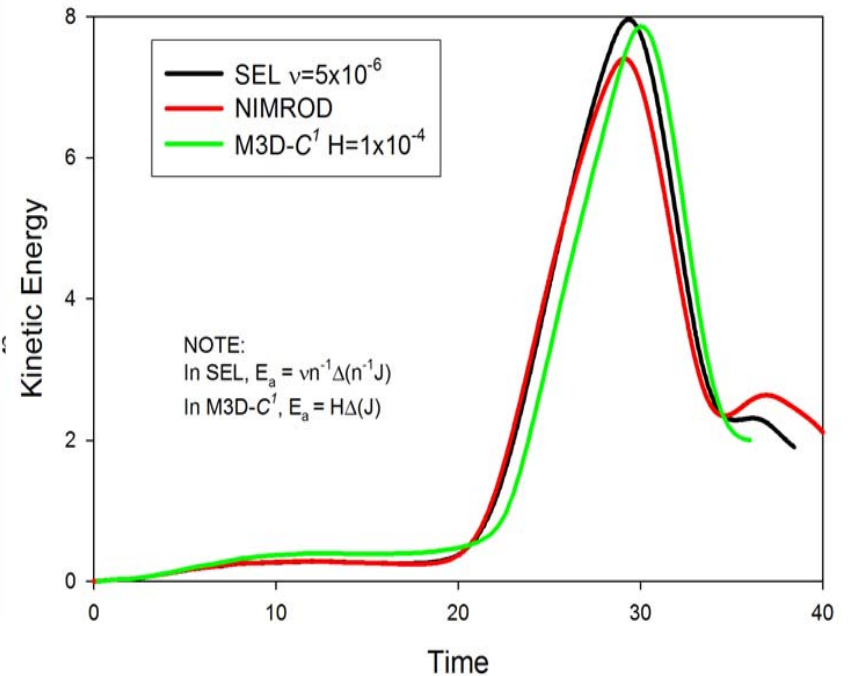
Initial and boundary conditions as in the original GEM challenge
(Birn, *et. al.*, J. Geophys. Res. **106**, 3715 (2001)):

$B_x = B_0 \tanh(y/\lambda)$, $\rho = \rho_0(1/\cosh^2(y/\lambda) + .2)$, $v_i = 0$, zero guide field, uniform temperature;
 $\lambda = d_i/2$; box size: $[l_x, l_y] = [25.6d_i, 12.8d_i]$, periodic in x, perfectly conducting walls in y.

SEL scan in electron viscosity



Comparison of K.E. vs time for 3 codes



Scalability By Domain Decomposition

- 3D extended MHD modeling of magnetically confined fusion plasmas requires petascale computing: 1 petaflop = 10^{15} flops $\sim 10^4$ procs.
- Efficient petascale computing requires scalable linear systems: condition number independent of grid size, number of processors.
- Domain decomposition is a promising approach to scalability.
 - Schwarz overlapping methods.
 - Non-overlapping methods, domain substructuring, *e.g.* FETI-DP.
- Analytical proofs of scalability for simple systems: Poisson, linear elasticity, Navier-Stokes.
- Empirical studies proposed using existing 2D SEL code for extended MHD.

FETI-DP

Finite Element Tearing and Interconnecting, Dual-Primal
Domain decomposition, non-overlapping, Schur complement

Axel Klawonn and Olof B. Widlund,
“Dual-Primal FETI Methods for Linear Elasticity,”
Comm. Pure Appl. Math. **59**, 1523-1572 (2006).

Partition

- I: Interior points, inside each subdomain (grid cell) Ω_j .
- Δ : Dual interface points, continuity imposed by Lagrange multipliers.
- Π : Primal interface points, continuity imposed directly.

Initial Block Matrix Form

$$\mathbf{L}\mathbf{u} = \mathbf{r}, \quad \mathbf{L} = \begin{pmatrix} \mathbf{L}_{II} & \mathbf{L}_{I\Delta} & \mathbf{L}_{I\Pi} \\ \mathbf{L}_{\Delta I} & \mathbf{L}_{\Delta\Delta} & \mathbf{L}_{\Delta\Pi} \\ \mathbf{L}_{\Pi I} & \mathbf{L}_{\Pi\Delta} & \mathbf{L}_{\Pi\Pi} \end{pmatrix}, \quad \mathbf{u} = \begin{pmatrix} \mathbf{u}_I \\ \mathbf{u}_\Delta \\ \mathbf{u}_\Pi \end{pmatrix}, \quad \mathbf{r} = \begin{pmatrix} \mathbf{r}_I \\ \mathbf{r}_\Delta \\ \mathbf{r}_\Pi \end{pmatrix}$$

Algebraic Reorganization

Local Block Matrices: $\mathbf{I} + \Delta$

$$\mathbf{L}_{BB} = \begin{pmatrix} \mathbf{L}_{II} & \mathbf{L}_{I\Delta} \\ \mathbf{L}_{\Delta I} & \mathbf{L}_{\Delta\Delta} \end{pmatrix}, \quad \mathbf{u}_B = \begin{pmatrix} \mathbf{u}_I \\ \mathbf{u}_\Delta \end{pmatrix}, \quad \mathbf{r}_B = \begin{pmatrix} \mathbf{r}_I \\ \mathbf{r}_\Delta \end{pmatrix}$$

Dual Continuity: Lagrange Multipliers

λ is a vector of Lagrange multipliers used to impose continuity on the dual dependent variables \mathbf{u}_Δ .

$$\mathbf{B} = \begin{pmatrix} \mathbf{0} & \mathbf{0} \\ \mathbf{0} & \mathbf{B}_\Delta \end{pmatrix}, \quad \mathbf{B}_\Delta \mathbf{u}_\Delta = 0, \quad \mathbf{L}_{BB} \mathbf{u}_B + \mathbf{L}_{B\Pi} \mathbf{u}_\Pi + \mathbf{B}^T \lambda = \mathbf{r}_B$$

Final Block Matrix Form

$$\mathbf{L} = \begin{pmatrix} \mathbf{L}_{BB} & \mathbf{L}_{B\Pi} & \mathbf{B}^T \\ \mathbf{L}_{\Pi B} & \mathbf{L}_{\Pi\Pi} & \mathbf{0} \\ \mathbf{B} & \mathbf{0} & \mathbf{0} \end{pmatrix}, \quad \mathbf{u} = \begin{pmatrix} \mathbf{u}_B \\ \mathbf{u}_\Pi \\ \lambda \end{pmatrix}, \quad \mathbf{r} = \begin{pmatrix} \mathbf{r}_B \\ \mathbf{r}_\Pi \\ \mathbf{0} \end{pmatrix}$$

Solution and Reduction

Solutions for \mathbf{u}_B and \mathbf{u}_Π

$$\mathbf{u}_B = \mathbf{L}_{BB}^{-1} \left(\mathbf{r}_B - \mathbf{L}_{B\Pi} \mathbf{u}_\Pi - \mathbf{B}^T \lambda \right)$$

$$\mathbf{S}_{\Pi\Pi} \equiv \mathbf{L}_{\Pi\Pi} - \mathbf{L}_{\Pi B} \mathbf{L}_{BB}^{-1} \mathbf{L}_{B\Pi}$$

$$\mathbf{u}_\Pi = \mathbf{S}_{\Pi\Pi}^{-1} \left[\mathbf{r}_\Pi - \mathbf{L}_{\Pi B} \mathbf{L}_{BB}^{-1} \left(\mathbf{r}_B - \mathbf{B}^T \lambda \right) \right]$$

Global Schur Complement Equation for λ

$$\mathbf{F} \lambda = \mathbf{d}$$

$$\mathbf{F} = \mathbf{B} \left(\mathbf{L}_{BB}^{-1} + \mathbf{L}_{BB}^{-1} \mathbf{L}_{B\Pi} \mathbf{S}_{\Pi\Pi}^{-1} \mathbf{L}_{\Pi B} \mathbf{L}_{BB}^{-1} \right) \mathbf{B}^T$$

$$\mathbf{d} = \mathbf{B} \mathbf{L}_{BB}^{-1} \left[\mathbf{r}_B - \mathbf{L}_{B\Pi} \mathbf{S}_{\Pi\Pi}^{-1} \left(\mathbf{r}_\Pi - \mathbf{L}_{\Pi B} \mathbf{L}_{BB}^{-1} \mathbf{r}_B \right) \right]$$

Solution Strategy

- Small dense block matrices of \mathbf{L}_{BB} solved locally by LAPACK.
- Sparse global, primal matrix \mathbf{S}_{III} solved in parallel by SuperLU_dist.
- Global Schur complement matrix \mathbf{F} solved by parallel preconditioned Krylov method, *e.g.* GMRES. Requires preconditioner for adequate rate of convergence.
- Choose primal interface constraints to provide coarse global problem, ensure scalability. 2D: vertices. 3D: more complicated.
- The scalability of \mathbf{F} is accomplished by the coarse, primal solver. The quality of the preconditioner determines the rate of convergence but not the scalability.
- Scalability has been proven analytically for a limited range of simple problems: Poisson, linear elasticity, Navier-Stokes. More general: empirical.

Preconditioning

Definitions For Each Subdomain Ω_i

$\mathbf{B}_{D,\Delta}^{(i)} \equiv$ scaled jump matrix

$\mathbf{R}_{\Gamma\Delta}^{(i)} \equiv$ restriction matrix from full interface to dual variables

$\mathbf{S}_{\varepsilon}^{(i)} \equiv$ Schur complement obtained by eliminating interior variables

Preconditioner

$$\mathbf{M}^{-1} = \sum_{i=1}^n \mathbf{B}_{D,\Delta}^{(i)} \mathbf{R}_{\Gamma\Delta}^{(i)} \mathbf{S}_{\varepsilon}^{(i)} \mathbf{R}_{\Gamma\Delta}^{(i)T} \mathbf{B}_{D,\Delta}^{(i)T}, \quad \mathbf{M}^{-1} \mathbf{F} \lambda = \mathbf{M}^{-1} \mathbf{d}$$

Condition Number

$$\mathbf{A} \mathbf{u}_i = \lambda_i \mathbf{u}_i, \quad \kappa(\mathbf{A}) \equiv \left| \frac{\lambda_{\max}}{\lambda_{\min}} \right|$$

Proposed Research Program

- Use existing 2D SEL spectral element code as test bed.
- Implement FETI-DP as a modification of existing static condensation routines.
- Study a progression of extended MHD systems as n_x and n_y are increased to determine:
 - Constancy of condition number.
 - Constancy of Krylov iterations required for convergence.
 - Scaling of condition number with parameters.
- Extend spectral element code to 3D.
- Investigate optimal choice of primal constraints for scalability.

Future Development of SEL

- Generalized domain connectivity and topology with PETSc Index Sets and Generalized Gather/Scatter
- Improved preconditioning and scalability by domain substructuring, FETI-DP.
- Third dimension of spectral elements.
- Slava Lukin: unstructured grid of triangles (2D) or tetrahedra (3D).
- Visualization with VisIt or AVS Express.
- CAD interface for input of geometry.

What Can SEL Contribute to M3D?

- Flux-source form.
- High-order C^0 spectral elements.
- Static condensation.
- Improved preconditioning and scalability by domain substructuring, FETI-DP.
- Harmonic grid generation.